Diffusion length of non-equilibrium minority charge carriers in β-Ga_2O_3 measured by electron beam induced current

E. B. Yakimov, A. Y. Polyakov, N. B. Smirnov, I. V. Shchemerov, Jiancheng Yang, F. Ren, Gwangseok Yang, Jihyun Kim, and S. J. Pearton

Citation: Journal of Applied Physics **123**, 185704 (2018); doi: 10.1063/1.5027559
View online: https://doi.org/10.1063/1.5027559
View Table of Contents: http://aip.scitation.org/toc/jap/123/18
Published by the American Institute of Physics

JOURNAL OF APPLIED PHYSICS **123**, 185704 (2018)

Diffusion length of non-equilibrium minority charge carriers in β-Ga_2O_3 measured by electron beam induced current

E. B. Yakimov,[1,2] A. Y. Polyakov,[1] N. B. Smirnov,[1] I. V. Shchemerov,[1] Jiancheng Yang,[3] F. Ren,[3] Gwangseok Yang,[4] Jihyun Kim,[4] and S. J. Pearton[5,a)]
[1]*National University of Science and Technology MISiS, 4 Leninsky Ave., Moscow 194017, Russia*
[2]*Institute of Microelectronics Technology and High Purity Materials, Russian Academy of Science, 6 Academician Ossipyan str., Chernogolovka, Moscow Region 142432, Russia*
[3]*Department of Chemical Engineering, University of Florida, Gainesville, Florida 32611, USA*
[4]*Department of Chemical and Biological Engineering, Korea University, Seoul 136-713, South Korea*
[5]*Department of Materials Science and Engineering, University of Florida, Gainesville, Florida 32611, USA*

(Received 3 March 2018; accepted 24 April 2018; published online 9 May 2018)

The spatial distribution of electron-hole pair generation in β-Ga_2O_3 as a function of scanning electron microscope (SEM) beam energy has been calculated by a Monte Carlo method. This spatial distribution is then used to obtain the diffusion length of charge carriers in high-quality epitaxial Ga_2O_3 films from the dependence of the electron beam induced current (EBIC) collection efficiency on the accelerating voltage of a SEM. The experimental results show, contrary to earlier theory, that holes are mobile in β-Ga_2O_3 and to a large extent determine the diffusion length of charge carriers. Diffusion lengths in the range 350–400 nm are determined for the as-grown Ga_2O_3, while processes like exposing the samples to proton irradiation essentially halve this value, showing the role of point defects in controlling minority carrier transport. The pitfalls related to using other popular EBIC-based methods assuming a point-like excitation function are demonstrated. Since the point defect type and the concentration in currently available Ga_2O_3 are dependent on the growth method and the doping concentration, accurate methods of diffusion length determination are critical to obtain quantitative comparisons of material quality. *Published by AIP Publishing.*
https://doi.org/10.1063/1.5027559

I. INTRODUCTION

There is significant recent interest in the recombination properties and trap populations in β-Ga_2O_3 because of the promise of this material for application in high-power rectifiers, solar-blind photodetectors and sensors.[1–7] The material can be readily grown both in the form of high-crystalline-quality bulk crystals and thick epitaxial films. It has a bandgap of ~4.9 eV, with a higher breakdown electric field than either GaN or SiC, and a high saturation velocity of electrons of 2×10^7 cm/s. Controllable n-type doping in a wide range of concentrations can be achieved by incorporating Sn or Si donors. Large area substrates are commercially available and various high-performance devices, such as Schottky diode rectifiers, field effect transistors with Schottky or isolated gates, and truly solar-blind photodetectors, have been demonstrated.[1–17]

One serious drawback of β-Ga_2O_3 is the lack of suitable shallow acceptor dopants. Theory[18,19] predicts all potentially viable acceptors in β-Ga_2O_3 to have large ionization levels. Moreover, the prediction is that, even if excited, for example, by illumination, the holes form virtually immobile polaronic states. However, recent experiments indicate that, at least at high temperatures, holes in β-Ga_2O_3 are mobile and can be supplied by Ga vacancy acceptors with levels close to $E_v + 1$ eV.[19] Moreover, recent measurements of nonequilibrium charge propagation using electron beam induced current (EBIC) and optical deep level transient spectroscopy (ODLTS) suggest that holes in β-Ga_2O_3 are mobile above room temperature.[20,21] It should be noted that the latter experiments have involved the injection of a non-equilibrium minority carrier population in n-type samples rather than holes obtained from p-type doping. The ability to transport holes in Ga_2O_3 has consequences for predicting the performance of the Ga_2O_3-based pn junction containing electronic and optoelectronic devices for which the knowledge of the diffusion length of nonequilibrium charge carriers is important. Moreover, it was shown in Refs. 20 and 21 that controlled introduction of point defects by either proton or electron irradiation degrades the minority carrier diffusion length. Deep level transient spectroscopy (DLTS) performed on bulk and epitaxial β-Ga_2O_3 have revealed several deep electron traps with energy levels near E_c-0.6 eV (E1), E_c-0.75 eV (E2), E_c-1.05 eV (E3), and Ec-1.2 eV (E4),[20,22–24] some of which were attributed to levels of transition metal impurities[21–23] or to native defects such as oxygen vacancies,[20,24] based on theoretical predictions.[25] Deep hole traps suggested to be related to gallium vacancy acceptors have been detected by electron paramagnetic resonance,[26] positron annihilation,[27] deep level optical spectroscopy (DLOS),[28] and ODLTS.[20] The concentrations of these traps vary depending on the growth method and the type and the concentration of doping. This is typical for newer wide bandgap materials, where the control of native and extrinsic defects is challenging.

Determining the diffusion length of the charge carriers in β-Ga_2O_3 and tracing the observed changes to the changes

[a)]Author to whom correspondence should be addressed: spear@mse.ufl.edu

in the type and the density of deep electron and hole traps are important to understanding the charge carrier recombination mechanism. The first step is to develop methods that allow the experimental determination of the diffusion lengths. Previously, we demonstrated for the case of another wide-bandgap material with short diffusion lengths, GaN,[28–30] that this can be obtained using EBIC. Combined with DLTS and ODLTS results for variously grown GaN films, this allowed assignment of the major deep electron traps that serve as lifetime killers in this material. A similar approach to that used in Ref. 28 to gain some insight into minority carrier transport in GaN is used here for Ga_2O_3. For β-Ga_2O_3, calculations of the electron-hole generation function as determined by the scanning electron microscope (SEM) probing beam energy in EBIC have not been reported and a critical analysis of EBIC measurements of diffusion lengths has not been presented. In this paper, we report the results of such calculations and apply the method to β-Ga_2O_3 films.

II. EXPERIMENTAL

Homoepitaxial β-Ga_2O_3 films were grown by hydride vapor phase epitaxy (HVPE) on bulk edge-defined-film-fed (EFG) β-Ga_2O_3 substrates with (001) orientation. The n^+ substrates were doped with Sn (net electron concentration of $3.6 \times 10^{18}\,cm^{-3}$), while the homoepitaxial films grown on these were doped with Si to net donor concentrations of 3×10^{15}–$4.6 \times 10^{16}\,cm^{-3}$. One of the films was also irradiated with a fluence of $10^{14}\,cm^{-2}$ of 10 MeV protons, as reported previously.[20] The substrates had a dislocation density below $10^3\,cm^{-2}$, as determined from etch pit counts.[20,32]

Diode samples were fabricated using full area Ti/Au backside Ohmic contacts. Front-side Schottky diodes with a diameter of 0.5 mm were fabricated by e-beam deposition of Ni/Au (20 nm of Ni and 60–80 nm of Au). EBIC measurements were performed using a field-emission scanning electron microscope (SEM) (JSM-6490, Jeol, Japan).[29–31] Preliminary results of deep trap and SEM measurements are described in Ref. 20. Those data showed the presence of traps at E_C–0.6 eV (concentration $\sim 3 \times 10^{13}\,cm^{-3}$), E_C–0.75 eV (concentration $\sim 5 \times 10^{13}\,cm^{-3}$), E_C-1.05 eV (concentration $\sim 2 \times 10^{14}\,cm^{-3}$) and E_C-2.3 eV (concentration $\sim 10^{15}\,cm^{-3}$) with minority carrier diffusion lengths in the range 350–380 nm. After irradiation with 10 MeV protons, this diffusion length dropped to 190 nm and a new trap at E_C–1.2 eV was observed.[20] In this paper, we use these samples to test the accuracy of various approaches to measuring the diffusion length in Ga_2O_{3+}.

III. RESULTS AND DISCUSSION

A. Diffusion length estimates from EBIC images of dislocations

Since the homoepitaxial material had a low dislocation density allowing for the detection of individual dislocations, we were able to detect individual dislocations as dark spots in EBIC images. Figure 1 shows an EBIC image taken with a probing beam accelerating voltage of 20 keV and a probing beam current of 0.1 nA for a SA diode with a drift layer carrier density of $4 \times 10^{16}\,cm^{-3}$. As shown in Refs. 29 and 33 for GaN, the diffusion length L can be roughly estimated from the full width at half maximum (FWHM) of the dislocation EBIC profile as FWHM = W + L/2, where W is the depletion region width. For the sample shown in Fig. 1, W $\sim$400 nm and FWHM $\sim$ 500–600 nm. That yields an estimate of the diffusion length as 100–200 nm. However, this is a very crude estimate because the FWHM also depends on the electron-hole pair generation volume. It does at least give the order of magnitude in agreement with a more accurate value of 300–350 nm obtained when using the planar-collector geometry, discussed in Sec. III B.

B. Diffusion length measurements based on monitoring the collected EBIC current dependence on the distance to the Schottky diode edge

For more precise measurements, the planar-collector geometry[34–36] can be used. In this method, the collected current I_c decay is measured on the collector-free surface as a function of distance x from the edge of a Schottky barrier or p-n junction perpendicular to the beam. This decay dependence on distance is the described in the point source approximation as[29]

$$I_c(x) = \exp(-x/L) \times x^{-n}, \tag{1}$$

with $n = 0.5$ for low surface recombination velocity ($s \to 0$) and $n = 3/2$ for $s \to \infty$.[34–36] However, as shown in Ref. 28, for materials with submicron diffusion length values, small beam energies should be used for correct measurements. To check if the beam energy is small enough, it was proposed in Ref. 33 to measure the collected current decay at different beam energies and determine if the same results are obtained. The collected current decay curves measured at a few beam energies together with fitting curves calculated using (1) with $n = \frac{1}{2}$ are shown in Figs. 2 and 3 for diodes with drift carrier densities of 4.6×10^{16} and $3 \times 10^{15}\,cm^{-3}$, respectively. The use of different carrier densities allows us to judge the sensitivity of diffusion length on this parameter

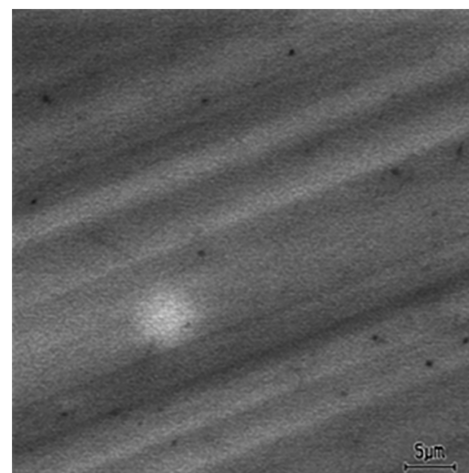

FIG. 1. EBIC image of a fragment of the β-Ga_2O_3 Schottky diode. Dislocations can be seen as dark dots.

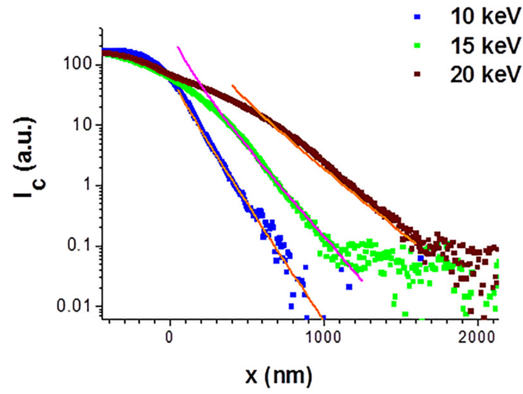

FIG. 2. $I_c(x)$ dependencies measured on a β-Ga_2O_3 Schottky diode with a drift layer carrier density of 3×10^{15} cm^{-3} in the planar-collector geometry at $E_b = 10$, 15 and 20 keV. The corresponding exp (-x/L)/$x^{0.5}$ dependencies are shown with solid lines.

and is particularly relevant to developing materials like Ga_2O_3. The characteristic I_c decay length strongly depends on beam energy. The effective diffusion length values are 120, 160, and 230 nm for the diode with a carrier density of 4.6×10^{16} cm^{-3} for E_b values of 10, 15, and 20 keV, respectively. For the diode with a drift region carrier density of 3 $\times 10^{15}$ cm^{-3}, the effective diffusion length values are 90, 150 and 350 nm for E_b equal to 10, 15 and 20 keV, respectively. This discrepancy in measured L values with different accelerating voltages makes the method described in this section highly inaccurate. However, the very existence of the EBIC decay profiles shown in Figs. 2 and 3 is very difficult to explain in any other way rather than assuming the injected holes to be mobile in β-Ga_2O_3, at least at room temperature.

C. The dependence of EBIC collection efficiency on the accelerating voltage of the probing beam

To obtain an accurate and reliable diffusion length value, another approach should be used. As discussed for GaN in Ref. 29, for the measurement of submicron diffusion length values, the method based on fitting the collected current dependence on beam energy[35,36] is most suitable. In this approach, for a sample with thickness much larger than L and using a Schottky barrier as a collector, the collected current I_c can be calculated numerically[37–40] knowing the distance from the irradiated surface, the normalized depth-dose dependence of the electron-hole generation rate and the three-dimensional electron-hole generation rate. The total number of electron-hole pairs created by the electron beam, the beam current and the fraction of beam energy absorbed inside the sample, the metal thickness and the average energy necessary for electron- hole pair creation are all part of this collected current. The functional dependence of the collected current can be calculated for β-Ga_2O_3 using the Casino Monte Carlo code.[40] The Monte Carlo calculation yields the depth dependence of energy deposition and the functional dependence described in Ref. 29, h(z). As a result, this function for Ga_2O_3 can be approximated as

$$h(z) = \frac{2.175}{R} \exp\left[-A\left(\frac{z}{R} - 0.16\right)^2\right], \tag{2}$$

where $R(\text{nm}) = 10 \cdot E_b(\text{keV})^{1.75}$ is the electron range and $A = \begin{cases} 24.5, z < 0.16 \cdot R \\ 7.3, z \geq 0.16 \cdot R. \end{cases}$

Figure 4 graphically presents the calculated electron range. The calculated electron range value is of much interest by itself because it is commonly used for estimating the generation volume dimensions.

In this approach, one needs to take into account the beam current losses due to the backscattering of the beam electrons and the energy losses in the metal of the Schottky diode. For thin metal layers, the reduced metal thickness $t_m = t \times \rho_{Ga2O3}/\rho_m$ (t is the actual metal thickness, ρ_{Ga2O3} and ρ_m are the Ga_2O_3 and metal densities, respectively) must be used and the generation function (2) can be used to extract the dependence of the collected current in the normal collector geometry. However, in our structures, the Schottky barrier thickness consisting of 20 nm Ni and 50–70 nm Au, was rather large. This effect can modify the collected current dependence on beam energy. Therefore, the energy deposition inside the Ga_2O_3 layer should be calculated for the multilayer structure related to the real geometry. Figure 5 illustrates the changes that can result from slightly varying the Au layer thickness of the Schottky barrier (from 50 nm to 70 nm), while keeping the Ni layer thickness constant at 20 nm. The variations are not dramatic, but measurable.

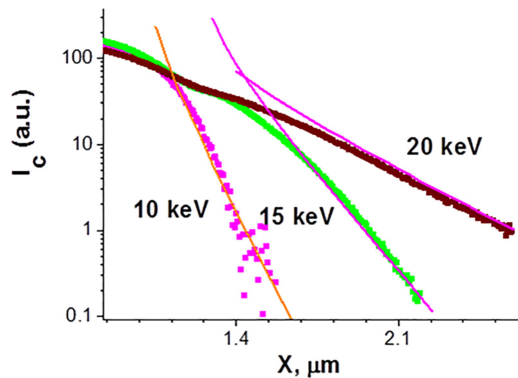

FIG. 3. $I_c(x)$ dependencies measured on a β-Ga_2O_3 Schottky diode with a higher drift layer carrier density of 4.6×10^{16} cm^{-3} in the planar-collector geometry at $E_b = 10$, 15 and 20 keV. The corresponding exp $(-x/L)/x^{0.5}$ dependencies are shown with solid lines.

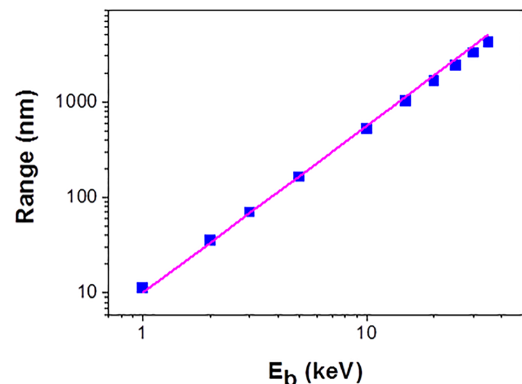

FIG. 4. The electron range dependence on E_b.

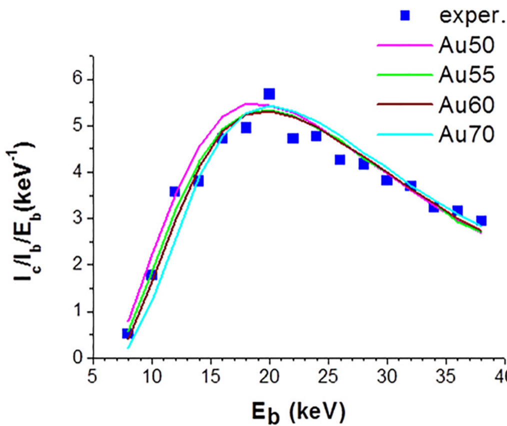

FIG. 5. The fitting procedure for a diode with a drift layer carrier density of 3×10^{15} cm^{-3}, as influenced by the actual thickness of the metal layer; solid blue squares are experimental points, the results of fitting are shown for the fixed net donor concentration of 3×10^{15} cm^{-3}, with the Ni layer kept at 20 nm thickness and the Au layer varied from: (1) 50 nm, (magenta curve, L = 420 nm) to (2) 55 nm (green curve, L = 420 nm), (3) 60 nm (brown curve, L = 400 nm), and (4) 70 nm (magenta curve, L = 360 nm); the best results are obtained when assuming the Au layer thickness to be 70 nm.

The diffusion length values obtained (i) when not taking into account the actual metal film thickness and (ii) taking the film thickness into account to find the value giving the best agreement with experiment do not seriously differ (10–20 nm in values of 350–380 nm). The estimated diffusion lengths are therefore only slightly affected by this dependence. The spatial variations of the net donor density (influencing the actual width of the space charge region) and the spatial variations of the density of deep traps that are the major lifetime killers can be taken into account for the fitting procedure if the relevant profiles are independently estimated from C-V and DLTS measurements. This could provide an independent check of the validity of the approximations. Such profiles could result from the influence of defects induced, for example, by polishing, dry etching of the surface or irradiation with low energy protons. Another attractive feature of the diffusion length calculation method outlined here is that, in contrast to the planar-collector geometry approach or worse still to measurements of photoconductivity decay times, the values of the diffusion lengths are not sensitive to assumptions regarding the surface recombination velocity.

IV. CONCLUSIONS

A comparison of different SEM-based approaches to determining the minority carrier diffusion length in Ga_2O_3 was carried out on the same samples. The most accurate, quantitative technique for determining the diffusion length of nonequilibrium charge carriers in β-Ga_2O_3 uses measurements of the collection efficiency of EBIC current as a function of the accelerating beam voltage. This has been used successfully previously in GaN, which also has small minority carrier diffusion lengths.[29] The electron-hole depth-dependent generation function and the dependence of the electron range on the electron energy for Ga_2O_3 have been calculated and relevant expressions closely approximating the results of numerical modeling using Monte Carlo simulations have been determined. Experimental measurements on homoepitaxial β-Ga_2O_3 films grown by HVPE on native β-Ga_2O_3 substrates using this most accurate approach show that the diffusion length is close to 400 nm but can be strongly decreased by controlled introduction of point defects using, for example, proton irradiation, which reduces the diffusion length by a factor of roughly two.[20]

ACKNOWLEDGMENTS

The work at NUST MISiS was supported in part by the Ministry of Education and Science of the Russian Federation in the framework of Increase Competitiveness Program of NUST «MISiS» (К2-2014-055). The work at IMT RAS was partially supported by the State task No. 007-01609-17-01. The work at UF was sponsored by the Department of the Defense, Defense Threat Reduction Agency, HDTRA1-17-1-011, monitored by Jacob Calkins. The work at Korea University was supported by a Korea University grant, LG Innotek-Korea University Nano-Photonics Program, Korea Institute of Energy Technology Evaluation and Planning (KETEP), and the Ministry of Trade, Industry and Energy (MOTIE) of the Republic of Korea (Grant No. 20163010012140).

[1] S. I. Stepanov, V. I. Nikolaev, V. E. Bougrov, and A. E. Romanov, "Gallium oxide: Properties and applications – A review," Adv. Mater. Sci. **44**, 63 (2016), available at http://www.ipme.ru/e-journals/RAMS/no_14416/06_14416_stepanov.pdf.
[2] H. von Wenckstern, Adv. Electron. Mater. **3**, 1600350 (2017).
[3] M. A. Mastro, A. Kuramata, J. Calkins, J. Kim, F. Ren, and S. J. Pearton, ECS J. Solid State Sci. Technol. **6**, P356 (2017).
[4] S. Rafique, L. Han, and H. Zhao, "Ultrawide bandgap β-Ga_2O_3 thin films: Growths, properties and devices," ECS Trans. **80**, 203 (2017).
[5] D. Gogova, G. Wagner, M. Baldini, M. Schmidbauer, K. Irmscher, R. Schewski, Z. Galazka, M. Albrecht, and R. Fornari, J. Cryst. Growth **401**, 665 (2014).
[6] A. Kuramata, K. Koshi, S. Watanabe, Y. Yamaoka, T. Masui, and S. Yamakoshi, Jpn. J. Appl. Phys., Part 1 **55**, 1202A2 (2016).
[7] S. J. Pearton, J. Yang, P. H. Cary IV, F. Ren, J. Kim, M. J. Tadjer, and M. A. Mastro, Appl. Phys. Rev. **5**, 011301 (2018).
[8] M. J. Tadjer, M. A. Mastro, N. A. Mahadik, M. Currie, V. D. Wheeler, J. A. Freitas, Jr., J. D. Greenlee, J. K. Hite, K. D. Hobart, C. R. Eddy, Jr., and F. J. Kub, J. Electron. Mater. **45**, 2031 (2016).
[9] J. Y. Tsao, S. Chowdhury, M. A. Hollis, D. Jena, N. M. Johnson, K. A. Jones, R. J. Kaplar, S. Rajan, C. G. Van de Walle, E. Bellotti, C. L. Chua, R. Collazo, M. E. Coltrin, J. A. Cooper, K. R. Evans, S. Graham, T. A. Grotjohn, E. R. Heller, M. Higashiwaki, M. S. Islam, P. W. Juodawlkis, M. A. Khan, A. D. Koehler, J. H. Leach, U. K. Mishra, R. J. Nemanich, R. C. N. Pilawa-Podgurski, J. B. Shealy, Z. Sitar, M. J. Tadjer, A. F. Witulski, M. Wraback, and J. A. Simmons, Adv. Electron. Mater. **4**, 1600501 (2018).
[10] S. Rafique, L. Han, M. J. Tadjer, J. A. Freitas, Jr., N. A. Mahadik, and H. Zhao, Appl. Phys. Lett. **108**, 182105 (2016).
[11] J. Kim, M. A. Mastro, M. J. Tadjer, and J. Kim, ACS Appl. Mater. Interfaces **9**, 21322 (2017).
[12] M. Higashiwaki, K. Sasaki, A. Kuramata, T. Masui, and S. Yamakoshi, Phys. Status Solidi A **211**, 21 (2014).
[13] M. J. Tadjer, N. A. Mahadik, V. D. Wheeler, E. R. Glaser, L. Ruppalt, A. D. Koehler, K. D. Hobart, C. R. Eddy, and F. J. Kub, ECS J. Solid State Sci. Technol. **5**, P468 (2016).
[14] A. J. Green, K. D. Chabak, E. R. Heller, R. C. Fitch, Jr., M. Baldini, A. Fiedler, K. Irmscher, G. Wagner, Z. Galazka, S. E. Tetlak, A. Crespo, K. Leedy, and G. H. Jessen, IEEE Electron Device Lett. **37**, 902 (2016).
[15] M. H. Wong, K. Sasaki, A. Kuramata, S. Yamakoshi, and M. Higashiwaki, IEEE Electron Device Lett. **37**, 212 (2016).
[16] S. Ahn, F. Ren, J. Kim, S. Oh, J. Kim, M. A. Mastro, and S. J. Pearton, Appl. Phys. Lett. **109**, 062102 (2016).

[17]J. B. Varley, A. Janotti, C. Franchini, and C. G. Van de Walle, Phys. Rev. B **85**, 081109 (2012).
[18]A. Kyrtsos, M. Matsubara, and E. Bellotti, Appl. Phys. Lett. **112**, 032108 (2018).
[19]E. Chikoidze, A. Fellous, A. Perez-Tomas, G. Sauthier, T. Tchelidze, C. Ton-That, T. T. Huynh, M. Phillips, S. Russell, M. Jennings, B. Berini, F. Jomard, and Y. Dumont, Mater. Today Phys. **3**, 118 (2017).
[20]A. Y. Polyakov, N. B. Smirnov, I. V. Shchemerov, E. B. Yakimov, J. Yang, F. Ren, G. Yang, J. Kim, A. Kuramata, and S. J. Pearton, Appl. Phys. Lett. **112**, 032107 (2018).
[21]J. D. Lee, E. Flitsiyan, L. Chernyak, J. Yang, F. Ren, S. J. Pearton, B. Meyler, and Y. J. Salzman, Appl. Phys. Lett. **112**, 082104 (2018).
[22]K. Irmscher, Z. Galazka, M. Pietsch, R. Uecker, and R. Fornari, J. Appl. Phys. **110**, 063720 (2011).
[23]Z. Zhang, E. Farzana, A. R. Arehart, and S. A. Ringel, Appl. Phys. Lett. **108**, 052105 (2016).
[24]M. E. Ingebrigtsen, J. B. Varley, A. Y. Kuznetsov, B. G. Svensson, G. Alfieri, A. Mihaila, U. Badstübner, and L. Vines, Appl. Phys. Lett. **112**, 042104 (2018).
[25]J. B. Varley, J. R. Weber, A. Janotti, and C. G. Van de Walle, Appl. Phys. Lett. **97**, 142106 (2010).
[26]B. E. Kananen, L. E. Halliburton, K. T. Stevens, G. K. Foundos, K. B. Chang, and N. C. Giles, Appl. Phys. Lett. **110**, 202104 (2017).
[27]E. Korhonen, F. Tuomisto, D. Gogova, G. Wagner, M. Baldini, Z. Galazka, R. Schewski, and M. Albrecht, Appl. Phys. Lett. **106**, 242103 (2015).
[28]A. A. Arehart, E. Farzana, T. E. Blue, and S. A. Ringel, paper presented at 2nd International Workshop on Ga2O3 and Related Materials, Parma, Italy, September 2017.
[29]E. B. Yakimov, J. Alloys Compd. **627**, 344 (2015).
[30]A. Y. Polyakov, N. B. Smirnov, E. B. Yakimov, S. A. Tarelkin, A. V. Turutin, I. V. Shemerov, S. J. Pearton, and I.-H. Lee, J. Alloys Compd. **686**, 1044 (2016).
[31]I.-H. Lee, A. Y. Polyakov, E. B. Yakimov, N. B. Smirnov, I. V. Shchemerov, S. A. Tarelkin, S. I. Didenko, K. I. Tapero, R. A. Zinovyev, and S. J. Pearton, Appl. Phys. Lett. **110**, 112102 (2017).
[32]G. Yang, S. Jang, F. Ren, S. J. Pearton, and J. Kim, ACS Appl. Mater. Interfaces **9**, 40471 (2017).
[33]P. S. Vergeles and E. B. Yakimov, J. Surf. Invest. X-ray, Synchrotron Neutron Tech. **3**, 58 (2009).
[34]D. E. Ioannou and C. A. Dimitriadis, IEEE Trans. Electron. Devices **29**, 445 (1982).
[35]H. K. Kuiken and C. van Opdorp, J. Appl. Phys. **57**, 2077 (1985).
[36]C. Donolato, Appl. Phys. Lett. **46**, 270 (1985).
[37]C. J. Wu and D. B. Wittry, J. Appl. Phys. **49**, 2827 (1978).
[38]J. Y. Chi and H. C. Gatos, J. Appl. Phys. **50**, 3433 (1979).
[39]E. Yakimov, Scanning Microsc. **6**, 81 (1992), available at https://www.scopus.com/record/display.uri?eid=2-s2.0-0026836285&origin=inward&txGid=e6992f5973ae83f544eb86dd5fa08cac.
[40]E. B. Yakimov and V. V. Privezentsev, J. Mater. Sci.: Mater. Electron. **19**, S277 (2008).